FIFTH INTERNATIONAL CONGRESS ON SOUND AND VIBRATION

DECEMBER 15-18, 1997
ADELAIDE, SOUTH AUSTRALIA

Invited Paper

ANALYSIS OF AN EXTENDED-TUBE THREE-PASS PERFORATED ELEMENT MUFFLER BY MEANS OF TRANSFER MATRICES

M.L. Munjal

Centre of Excellence for Technical Acoustics,
Department of Mechanical Engineering,
Indian Institute of Science,
Bangalore 560 012,
India

Abstract

A majority of the present-day automobile exhaust systems make use of three-pass mufflers that are characterized by low back pressure and good acoustic performance because of interaction of waves in the three pass tubes with those in the annulus. A frequency-domain one-dimensional transfer matrix model is presented here for an extended-tube three-pass perforated element muffler. Transmission loss values computed therefrom have been shown to reduce to those of the flush-tube configuration in the limit. Finally, results of parametric studies are reported in order to help muffler designers in synthesizing an efficient muffler configuration within a given overall length of the chamber.

INTRODUCTION

Three-pass mufflers (see Fig.1) have the advantage of good acoustic performance coupled with low back pressure. Therefore, these have been used on automobile exhaust system for several years. However, their design has been empirical by and large. Dickey et al. numerically analysed such a muffler[1], where waves in the three inner perforated ducts interact with waves in the annulus, as shown in Figs.1 and 2. Their predictions of transmission loss tallied very well with the experimentally observed values for stationary medium in the plane wave frequency range.

Recently, the frequency-domain transfer matrix approach of Ref. 2 has been extended to the flush tube three-pass perforated element muffler shown in Fig.1, where waves in four ducts (three pass tubes and the engulfing chamber) interact with each other[3]. Transmission loss values computed from the resulting transfer matrices are compared with those computed by means of a numerical approach by Dickey et al[1], which in turn have been verified experimentally for stationary medium. This approach has been extended in the present paper to the extended-tube three-pass perforated element configuration shown in Fig. 3.

A TRANSFER MATRIX MODEL

In the common portion of length l, there is an interaction of waves in four ducts, viz three perforated ducts (of diameters d_1, d_2 and d_3) and the annular space in the shell of (equivalent) diameter d_4, as shown in Fig. 2. Basic equations of mass continuity, momentum balance and energy for these four ducts may be written as in Ref. 2, making use of the following assumptions:

(a) mean flow in the annular space is zero, i.e., $U_4 = 0$;
(b) mean flows in the perforate ducts numbered 1, 2 and 3 are of grazing nature; i.e., there is no flow through the perforations ;
(c) radial velocities are all positive from inside to outside ;
(d) wall thickness of the perforated ducts is negligible ;
(e) numerical value of U_2 will be negative ;
(f) the mean flow is incompressible ; and
(g) the waves are linear.

Assumption (b) follows from the experimental observation of Gogate and Munjal[4] that there is a natural tendency of the mean flow to take the easier path of grazing the perforations rather than passing across (or through) the holes.

Working in the frequency domain, time dependence of all state variables may be assumed to be harmonic ($e^{j\omega t}$).

Making use of the generalized de-coupling analysis of Refs 2 and 5, or the eigenvalue analysis of Ref. 6, the following transfer matrix equation has been derived in Ref. 3:

$$\begin{bmatrix} S_1(o) \\ S_2(o) \\ S_3(o) \end{bmatrix} = \begin{bmatrix} D & E & F \\ G & H & K \\ P & Q & R \end{bmatrix} \begin{bmatrix} S_1(l_p) \\ S_2(l_p) \\ S_3(l_p) \end{bmatrix} \qquad (1)$$

where

$$\{S_i\} = [p_i \quad V_i]^T$$

and D, E, F, G, H, K, P, Q and R are 2x2 sub-matrices. Explicit expressions for elements of all these sub-matrices have been derived in Ref. 3.

Now, state variables at $z = l_p$ in duct 1 may be related to those in duct 2 across the right end cavity in Fig. 3 by means of the transfer matrix relation:

$$\{S_1(l_p)\} = [A] \ \{S_2\ (l_p)\} \qquad (2)$$

where [A] is product of the transfer matrices of

(a) a duct of length $\delta_1 + l_{4b} + t_b + l_1$,
(b) reversal expansion element,
(c) extended outlet element, and
(d) a duct of length $\delta_2 + t_b + l_{4b} + l_{2b}$

All these matrices have been derived in Ref. 2 and were available to the author as subroutines. Here, δ_1 and δ_2 are end corrections. These may be adopted from Ingard's paper[7], replacing the infinite flange end correction of 0.85 r by the corresponding value for a free and (0.6 r) that would be more appropriate for a perforated tube. Thus,

$$\delta_1 = ecf\,(0.6\,r_1)(1 - 1.25\,r_1 / r_b) \qquad (3)$$

$$\delta_2 = ecf\,(0.6\,r_2)(1 - 1.25\,r_2 / r_b) \qquad (4)$$

where

$$r_b = (r_4^2 - r_3^2)^{1/2}$$
$$r_1, r_2, r_3, r_4 = (d_1, d_2, d_3, d_4)/2$$

ecf is the end correction fraction, which may vary from 0 to 1, because Ingard's expressions for end corrections are not for perforated pipes. However, ecf=1.0 has been shown to yield the best corroboration with experimental results in Refs. 1 and 3.

Similarly, state variables at z=0 in duct 2 may be related to those in duct 3 across the left end cavity by means of the relation:

$$\{S_2(o)\} = [B] \ \{S_3(o)\} \qquad (5)$$

where [B] is product of the transfer matrices of

(a) a duct of length $\delta_2 + l_{4a} + t_a + l_{2a}$
(b) reversal expansion element
(c) extended outlet element
(d) a duct of length $\delta_3 + l_3 + t_a + l_{4a}$

where δ_1 is given by Eq. (3) above, and

$$\delta_3 = ecf\,(0.6\,r_3)(1 - 1.25\,r_3 / r_a) \qquad (6)$$

with

$$\bar{r}_a = (r_4^2 - r_1^2)^{1/2}, \text{ and ecf} = 1.$$

Matrix equations (1), (2) and (5) may now be combined to obtain the transfer matrix relation for the entire chamber (see Fig.3):

$$\{S_1(o)\} = [[D][A][W] + [E][W] + [F]]\,\{S_3(l_p)\}$$

$$\equiv [C]\,\{S_3(l_p)\} \qquad (say) \qquad (7)$$

where

$$[W] = [[G][A] + [H] - [B][P][A] - [B][Q]]^{-1}[[B][R] - [K]] \qquad (8)$$

and

$$[C] = [D][A][W] + E[W] + [F] \qquad (9)$$

The overall transfer matrix [C] can now be combined with the upstream and downstream pipe elements, and transmission loss can be evaluated from the four-pole parameters of the entire muffler (see for example Refs. 2 - 5).

PARAMETRIC STUDIES

Dimensions of the configuration of Fig. 3 are :

$l_a = 0.07$ m , $l_p = 0.2$ m, $l_b = 0.1$ m, $l_{4a}=l_{4b}=0.0055$ m,
$t_a = t_b = 0.002$ m, porosities $\sigma_1 = \sigma_2 = \sigma_3 = 0.05$,
radii $r_1 = r_2 = r_3 = 0.0246$ m, $r_4 = 0.0825$ m,
wall thicknesses $th_1 = th_2 = th_3 = 0.0008$ m,
hole diameters $dh_1 = dh_2 = dh_3 = 0.0025$ m,
and the mean flow Mach number $M_1 = M_2 = M_3 = 0.1$.

Besides, medium density $\rho_o = 1.18$ kg/m^3 and sound speed $a_o = 344$ m/s .

The generalized muffler program in FORTRAN developed over the years has been extended incorporating subroutines that return transfer matrix of the extended-tube three-pass configuration to the MAIN program. This transfer matrix is then combined with those of the upstream and downstream elements to obtain an overall or product transfer matrix for the entire muffler. Transmission loss may then be calculated from the four-pole parameters of the overall transfer matrix.

In order to help muffler designers in appreciating and exploiting the behaviour of three-pass mufflers, on the lines of Ref. 3 and 8, some parametric studies are reported in Figs.4 to 6 in order to demonstrate the effect of the extended tube lengths tabulated hereunder.

Table: Extended Tube Lengths

		l_1	l_{2a}	l_{2b}	l_3
Fig. 4	(a)	0	0	0	0
	(b)	0.03	0.02	0	0
	(c)	0.06	0.04	0	0
Fig. 5	(a)	0	0	0	0
	(b)	0	0	0.03	0.02
	(c)	0	0	0.06	0.04
Fig. 6	(a)	0	0	0	0
	(b)	0.03	0.02	0.06	0.04
	(c)	0.06	0.04	0.03	0.02

It may noted from Figs. 4, 5 and 6 that the effect of the extension of inlet and outlet tubes into the end cavities is marginal and of no particular significance to designers. However, small extensions may be unavoidable for exigencies of fabrication, and may be analysed by means of transfer matrices as indicated above.

CONCLUDING REMARKS

The model presented in this paper brings extended-tube three-pass perforated-element chamber mufflers in line with other elements for analysis of mufflers on computer. There is, however, a major limitation in that all the three pass tubes have been assumed to be perforated to the same length so that a common perforated section could be considered in the analysis. This assumption may not hold for some commercial muffler configurations which have been developed empirically.

ACKNOWLEDGEMENTS

The investigation reported here has been made possible by the financial support of the Centre of Excellence for Technical Acoustics by Department of Science and Technology of the Government of India.

REFERENCES

[1]Dickey, N. S., Selamet A., and Novak, J. M., J. Sound Vib. (to appear in 1997) Multi-pass perforated tube silencers: a computational approach.

[2]Munjal, M. L., Acoustics of Ducts and Mufflers, Wiley-Interscience, New York, (1987).

[3]Munjal, M.L., Analysis of a flush-tube three-pass perforated element muffler by means of transfer matrices, International Journal of Acoustics and Vibration 2(2), (1997).

[4]Gogate, G. R., and Munjal, M. L., Analytical and experimental aeroacoustic studies of open-ended three-duct perforated elements used in mufflers, J. Acoust. Soc. Am. **97**, 2919-2927 (1995)

[5]Munjal, M. L., Rao, K. N., and Sahasrabudhe, A. D., Aeroacoustic analysis of perforated muffler components, J. Sound Vib. **114**(2), 173-188 (1987)

[6]Peat, K. S., A numerical decoupling analysis of perforated pipe silencer elements, J. Sound Vib. **123**(2), 199-212 (1988)

[7]Ingard, U., On the theory and design of acoustic resonators, J. Acoust. Soc. Am. **25**(6), 1037-1061 (1953)

[8]Munjal, M. L., Krishnan, S., and Reddy, M. M., Flow-acoustic performance of the perforated elements with application to design, Noise Control Eng. J., **40**(1), 159-167 (1993).

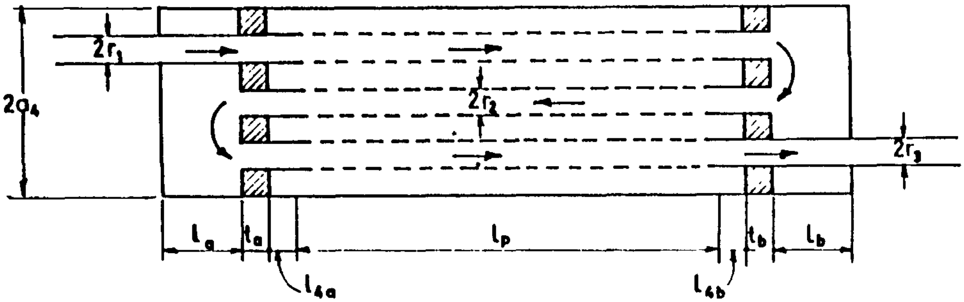

Fig.1. A functional sketch of a flush-tube three-pass perforated element chamber

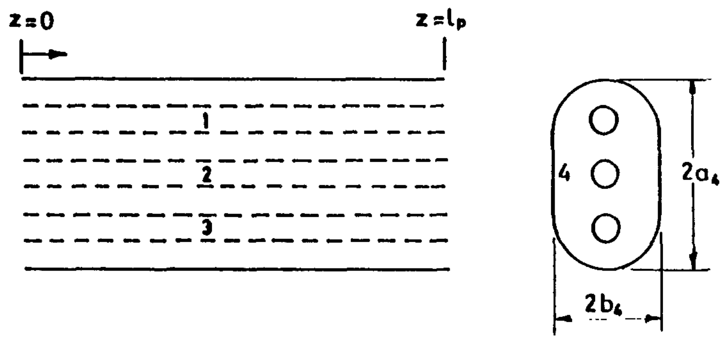

Fig. 2. Interaction of waves in the common perforated portion ($r_4^2 = a_4 b_4$)

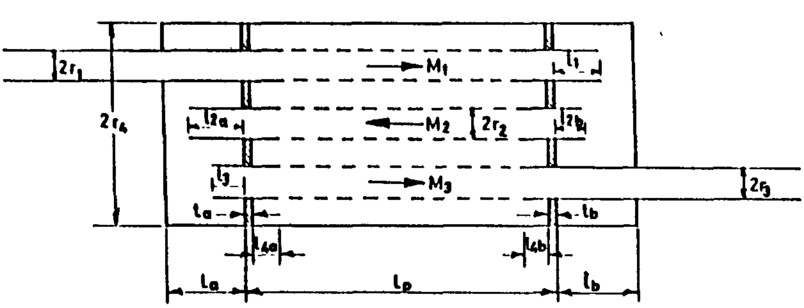

Fig.3. A functional sketch of the extended-tube three-pass perforated element chamber

Fig 4. Effect of extended inlet tubes, with outlet tubes being flush with the three-pass chamber.

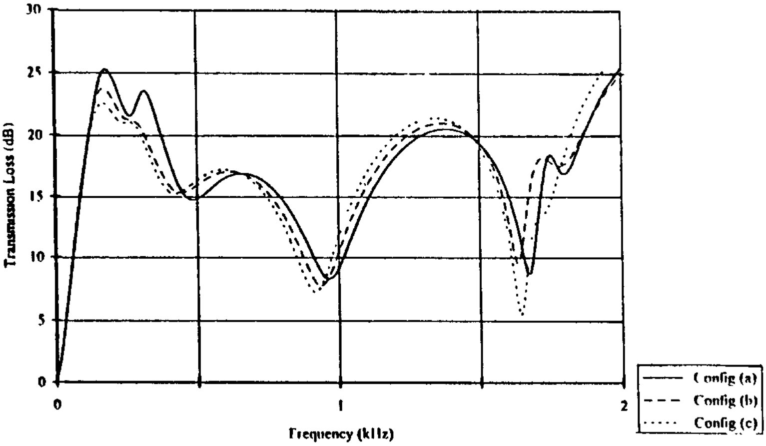

Fig 5. Effect of the extended outlet tubes, with the inlet tubes being flush with the three-pass chamber.

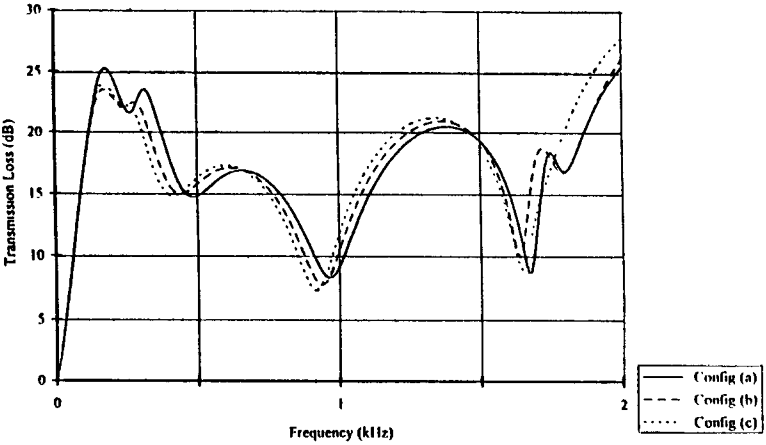

Fig 6. Effect of differences in the lengths of the extended inlet/outlet tubes.